Received: 3 August 2022 | Accepted: 4 August 2022

DOI: 10.1002/jccs.202200347

JCCS JOURNAL OF THE CHINESE CHEMICAL SOCIETY

REVIEW

Computational studies on the excited state decay rates in aggregates of two-coordinate Cu (I) complexes: Thermally Activated Delayed Fluorescence and Aggregation Induced Emis

Shiyun Lin[1] | **Qi Ou**[2] | **Qian Peng**[3] | **Zhigang Shuai**[1,4]

[1]MOE Key Laboratory of Organic OptoElectronics and Molecular Engineering, Department of Chemistry, Tsinghua University, Beijing, P. R. China

[2]AI for Science Institute, Beijing, P. R. China

[3]School of Chemical Sciences, University of Chinese Academy of Sciences, Beijing, P. R. China

[4]School of Science and Engineering, The Chinese University of Hong Kong, Shenzhen, P. R. China

Correspondence
Zhigang Shuai, MOE Key Laboratory of Organic OptoElectronics and Molecular Engineering, Department of Chemistry, Tsinghua University, Beijing 100084, P. R. China.
Email: zgshuai@tsinghua.edu.cn

Funding information
National Natural Science Foundation of China, Grant/Award Numbers: 21788102, 22003030; Ministry of Science and Technology of China through the National Key R&D Plan, Grant/Award Number: 2017YFA0204501

Abstract

Two-coordinate Cu (I) complexes have attracted great interest recently because of the rich photophysical property in solid state, including the aggregation-induced thermal activated delayed fluorescence. Here, we summarize our theoretical investigations on the excited state structure and decay dynamics for the two-coordinate Cu (I) complexes in solution phase and solid state by the thermal vibration correlation function rate formalism we developed earlier coupled with time-dependent density-functional theory within polarizable continuum model and hybrid quantum and molecular mechanics. First, for the CAAC—Cu (I)—Cl complex, we found that the nature of the excited state undergoes a change from metal-to-ligand charge transfer (MLCT) in solution to hybrid halogen-to-ligand charge transfer and MLCT in solid state. The bending vibrations of the C—Cu—Cl and Cu—C—N bonds are restricted in aggregates, reducing the non-radiative decay rate to cause strong solid-state fluorescence. Second, for CAAC—Cu (I)—Cz, we found that both intersystem crossing (ISC) and reverse intersystem crossing (rISC) are enhanced by 2–4 orders of magnitudes upon aggregation, leading to highly efficient thermally activated delayed fluorescence (TADF). The enhanced ISC and rISC rates can be attributed to the increase of the metal proportion in the frontier molecular orbitals, leading to an enhanced spin−orbit coupling between S_1 and T_1. The reaction barriers for ISC and rISC are much lower in solution than that in aggregate phase resulting in a decrease in energy gap ΔE_{ST} and an increase in the relative reorganization energy through bending the angle $\angle C-Cu-N$ for T_1. Our theoretical studies provide a clear rationalization for the highly efficient solid-state luminescence character of two-coordinate Cu (I) complexes and may clarify the ongoing dispute on the understanding of the high TADF quantum efficiency.

KEYWORDS

aggregation-induced emission (AIE), QM/MM, thermal vibration correlation function (TVCF), thermally activated delayed fluorescence (TADF), two-coordinate Cu(I) complex

1 | INTRODUCTION

In the past decades, copper complexes have attracted great attention for the potential to replace rare metals in organic light-emitting diodes (OLEDs) application.[1–3] Compared with traditional phosphorescent noble metal complexes, copper complexes exhibit a series of advantages, including abundance in nature, low cost, easy access, versatile coordination forms, etc. Especially, the optical emission can be tuned from fluorescence to phosphorescence and from blue to red. Since 1980, McMillin have extensively studied solid-state luminescence of $[Cu(phen)(PPh_3)_2]$.[4] Nevertheless, searching for highly efficient luminescent copper complexes is still a key challenge of organic luminescence.

In 2001, Tang et al. put forward the concept of aggregation-induced emission (AIE) to describe the exotic phenomenon of organic chromophores demonstrating a substantial increase in luminescence upon aggregation,[5] broadening the vision to design high-efficiency solid-phase organic system. The AIE-active systems have shown a great diversity ranging from fluorescent oligomers to phosphorescent organometallic complexes.[6,7] Since the geometric distortion of copper complexes in excited state usually enhances non-radiative decay,[2] the exploration of the luminescence mechanism in Cu(I) complex aggregates is crucial to its molecule design.

In general, copper has two types of oxidation states: Cu(I) and Cu(II). The outermost shell electron configuration of Cu(II) is d^9, which allows d-d* electron transition to form the metal center (MC) state.[2,8] The MC state usually accompanies severe structural deformation and induces the excited state deactivation.[9] Hence, the luminescence of Cu(II) complexes is always weak.[10] Unlike Cu(II) complexes, the outermost d orbitals of Cu(I) complex is full, avoiding any d-d* transition and formation of MC state. Spin-orbit coupling (SOC) of copper complexes is much smaller than traditional phosphorescent heavy metal complexes, and copper complexes can achieve both singlet and triplet harvest in consequence.[2] Therefore, copper complexes can give rise to prompt fluorescence,[11] phosphorescence,[12] and delayed fluorescence[13] under different circumstances.

Cu(I) complexes possess a number of coordination structures, such as four-coordinate tetrahedral,[14] three-coordinate trigonal planar,[12] and two-coordinate linear structures.[15] These lead to a wide range of emission spectra. Upon photo-excitation, the MC is transiently oxidized to a d^9 configuration, which consequently induces pseudo-Jahn–Teller (PJT) distortion in copper complex (Figure 1).[2,10] Four-coordinate Cu(I) complexes unfortunately suffer from the PJT effect upon excitation, which always induces geometric planarization in the excited state and leads to extra non-radiative decay.[4] Similarly, PJT distortion is also found

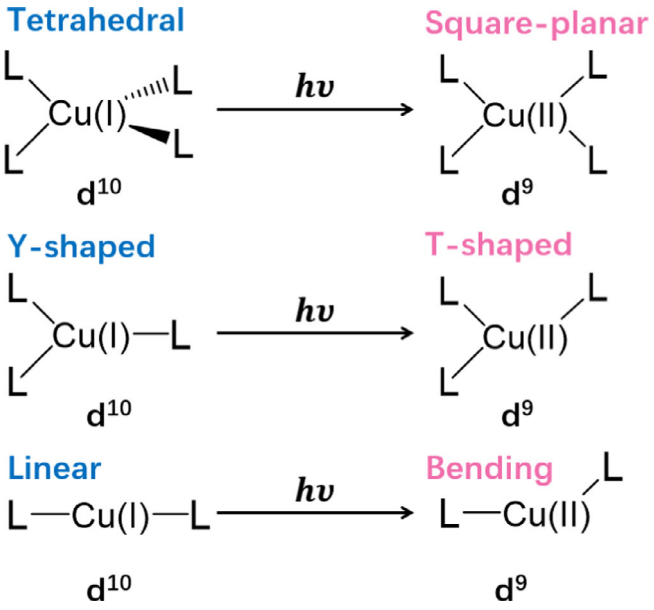

FIGURE 1 Pseudo-Jahn–Teller distortion of Cu(I) complexes upon excitation

in three-coordinate Cu (I) complex, with a "Y"-shaped to "T"-shaped structural reorganization.[16] The novel two-coordinate Cu(I) complexes show high performance in OLED, which have attracted great attention.[3,15] However, the photo-excited linear two-coordinate Cu(I) complex can also decay non-radiatively through a geometric bending deformation, known as Renner–Teller distortion.[17] It is of great interest to look at the photophysical properties for two-coordinate Cu(I) complexes in aggregate phase.

Blasse et al.[4] observed thermally activated delayed fluorescence (TADF) luminescence in Cu(I) complexes which were applied in OLEDs by Peters et al.[18] later, demonstrating external quantum efficiency (EQE) as high as 16.1%. Recently, two-coordinate Cu(I) complexes have attracted much attention owing to its highly efficient TADF. The novel complexes can achieve photoluminescence efficiencies >99% and microsecond lifetimes,[15] which has made a great breakthrough in the study of Cu(I) complexes.

Although the luminescent performance of Cu(I) complexes has been dramatically improved, the luminescence mechanism is still under debate. Hence, comprehensively studying the photophysical process of Cu(I) complex in aggregates and revealing the mechanism is essential. Herein, we systematically and quantitatively investigated the excited-state decay dynamics in two-coordinate Cu(I) complexes in solution and aggregates by combining the polarizable continuum model (PCM)[19] and hybrid quantum and molecular mechanics (QM/MM)[20] approach with thermally vibrational correlation function (TVCF) formalism[21–23] we developed

earlier. It is important to point out that Professor Sheng-Hsien Lin is a pioneering figure for the molecular radiationless decay theory based on Fermi golden rule already dated back to 1966 and thereafter.[24,25] The novelty of our TVCF lies in three aspects: (a) all the vibrational modes could serve as non-adiabatic coupling prefactor, instead of one specific mode assumed a priori; (b) time-dependent formalism allowing fully analytical solutions for both displaced and Duschinsky rotation mixing all the modes and a Fast Fourier transformation (FFT) technique can be employed to reduce the computational scaling; (c) and SOC term has been introduced. In addition, a computational software MOMAP (Molecular Materials Property Prediction Package) has been developed for general users which gained quite some popularity.[26]

According to Lin,[27] the non-adiabatic coupling term can be expressed as follows: $R_l(fi) = -\hbar^2\langle\Phi_f\left|\frac{\partial}{\partial Q_l}\right|\Phi_i\rangle$. Here, Φ is the electronic state and Q is the vibrational mode coordinate and l is the so-called "promoting mode," which is easily identified for small system. But for polyatomic molecule, many modes could also contribute. We have formulated a general rate formulism by which all the modes could serve as "promoting mode":

$$W_{f\leftarrow i}(T) = \frac{2\pi}{\hbar}\sum_{l,k} R^f_{lk}\frac{1}{Z_{iv}}\sum_{v_i,v_f} e^{-\beta E_{iv_i}}\Omega^f_{lk}\delta\left(E_{fi}+E_{fv_f}-E_{iv_i}\right), \quad (1)$$

where the non-adiabatic prefactor R now becomes a matrix indexed by l and k instead of only one mode $R^f_{lk} = \langle\Phi_f\left|\widehat{P}_{fl}\right|\Phi_i\rangle\langle\Phi_i\left|\widehat{P}_{fk}\right|\Phi_f\rangle$ and Ω is expressed as follows:

$$\Omega^f_{lk} = \langle\Theta_{fv_f}\left|\widehat{P}_{fl}\right|\Theta_{iv_i}\rangle\langle\Theta_{iv_i}\left|\widehat{P}_{fk}\right|\Theta_{fv_f}\rangle, \quad (2)$$

where P is the vibrational momentum operator and Θ is the vibrational wavefunction. We further introduced the Duschinsky rotation effect as follows:

$$Q_{ik} = \sum_{l}^{3n-6} S_{i\leftarrow f,kl}Q_{fl} + \underline{D}_{i\leftarrow f,k}, \quad (3)$$

where S is Duschinsky rotation matrix to express vibrational mode as a linear combination of another manifold and D is the vibrational displacement vector.

By Fourier transforming the delta function in Equation (1) and employing continuously the completeness relationship for the vibrational modes basis, and expressing Equation (3).

$\langle\underline{x}'|\underline{x}\rangle = \delta\left[\underline{x}' - (S\underline{x}+\underline{D})\right]$ along with the nuclear momentum P matrix element expressed as $\langle x_k\left|\widehat{P}_{fk}\right|y_k\rangle = -i\hbar\frac{\partial}{\partial x_k}\delta(x_k - y_k)$, we have been able to obtain an analytical expression of rate as time integration. The computational cost scales simply as N^3 for each time step (N is the number of vibrational modes). And the time integration can be computed very efficiently by FFT technique which happened to have experienced a rapid development in the past years.

As a matter of fact, we have sent the preprint of the work[22] to Prof. Sheng-Hsien Lin for his advice. He immediately replied: "... the manuscript 'Promoting-mode free formalism for excited state radiation less decay process with Duschinsky rotation effect' ... deeply impressed, ... This is certainly a landmark paper in the field of excited state radiationless decay theory..." These words are highly encouraging for us which led to a series of continued work on revealing the excited state processes and light-emitting phenomena. We have unraveled the mechanism for the highly efficient fluorescence[17] and TADF[27] of two Cu(I) complexes in solid state by employing the TVCF method and we will present the summary here.

2 | AIE INDUCED BY RESTRICTION OF COORDINATION BOND BENDING IN TWO-COORDINATE Cu(I) COMPLEXES

We first studied (CAAC^{Ad})CuCl (see Figure 2a), which has been reported to exhibit strong blue solid-state fluorescence with photoluminescence quantum yield (PLQY) up to 96%.[11] Geometry optimization and electronic structures for the ground state and the lowest-lying excited singlet state were carried out by (TD)M06/6-31G (d)/LANL2DZ approach with PCM for tetrahydrofuran (THF) solvent to account for the solvent effect and ONIOM model[28] with universal force field (UFF) to model the solid environment. The linear-response (LR) PCM[19] was employed for the geometrical optimization and frequencies analysis, while the corrected linear-response (cLR)[29] approach was employed to obtain excitation energies. Herein, the central molecule was treated as QM part using (TD)M06/LANL2DZ/6-31G (d) and the surrounding molecules were treated as MM part using the UFF. All these first-principle calculations were carried out with *Gaussian16* program package.[30]

Based on the optimized geometry of S_0 and S_1 states of (CAAC^{Ad})CuCl in solution and solid phases, we found that the largest geometry modifications appear in the coordination bond angles between copper and two ligands with ∠C1—Cu—Cl, ∠Cu—C1—N, and ∠Cu—C1—C4 decreasing from 9.67°, 12.82° and 10.73° in solution to 3.66°, 4.46° and 6.75° in solid phase, respectively. These changes lead to distinctly different electronic structure and non-radiative decay rate. It can be

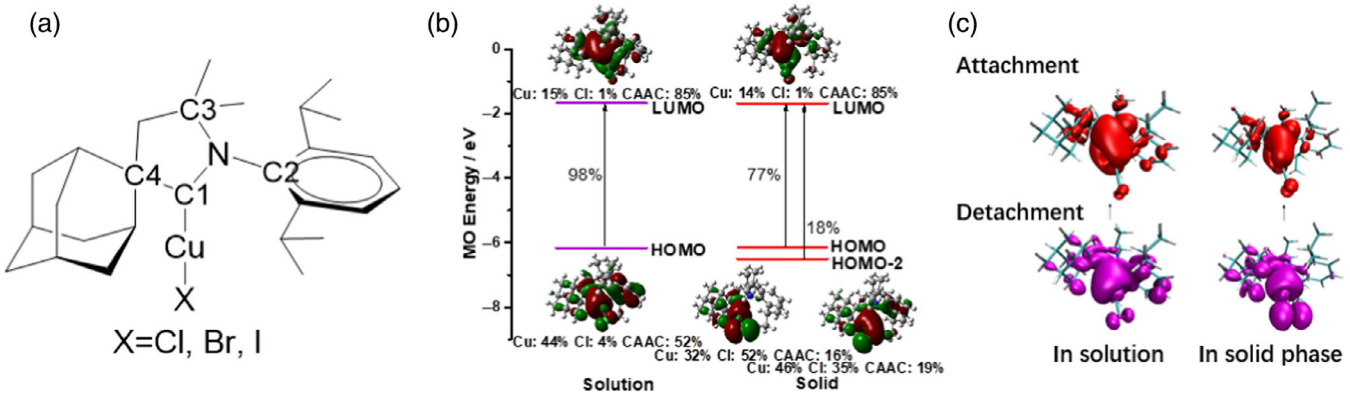

FIGURE 2 (a) Chemical Structure of (CAAC^{Ad})CuX; (b) Selected frontier molecular orbitals and the important transitions of the S_1 state at the optimized S_1 geometries in solution and solid phase; (c) Attachment-detachment electron densities for S_1 states at their optimized geometries in solution and solid state. Reproduced with permission from ref. [17]. Copyright 2019 American Chemical Society

TABLE 1 The calculated oscillator strength, vertical excitation energy, radiative (k_r), non-radiative (k_{nr}) and intersystem crossing (k_{isc}) decay rates constants, fluorescence quantum yield of (CAAC^{Ad})CuCl in solution and solid phase at 298 K

	f	ΔE (eV)	k_r (s^{-1})	k_{ic} (s^{-1})	k_{isc} (s^{-1})	Φ_F (%)
In solution	0.0030	2.87	6.26×10^5	8.38×10^7	9.18×10^2	0.44
In solid state	0.0024	2.95	7.83×10^5	1.47×10^4	1.21×10^2	98.0

Note: Reproduced with permission from ref. [17]. Copyright 2019 American Chemical Society.

seen from Figure 2b that the nature of excitation changes from metal-to-ligand charge transfer (MLCT) to hybrid MLCT and halogen-to-ligand charge transfer (XLCT) upon aggregation. Consequently, the excitation energy increases from 2.88 to 2.95 eV due to the participation of the deeper molecular orbitals in the solid state, which is confirmed by the blue shift of the experimental emission spectrum with respect to that in solution. The attachment-detachment electron densities were analyzed by Q-Chem Package,[31] and it is evident that the electron transitions can be assigned to MLCT in solution, and mixing MLCT/XLCT in solid phase.

Based on the ab initio calculations, we calculated the radiative and non-radiative decay rate constants of (CAAC^{Ad})CuCl in solution and solid phase using MOMAP package[26] as Table 1 shown. From Table 1, it can be seen that from solution to solid phase both oscillator strength and adiabatic excitation energy barely change. Thus, the radiative decay rate constants are close in both phases. Contrarily, upon aggregation, the non-radiative internal conversion rate constant k_{ic} decreases by about four orders of magnitude, and the resultant fluorescence quantum yield (Φ_F) increases from 0.44 to 98% upon aggregation, which is very close to the experiment value of 96% in solid state.

As discussed above, the internal conversion rate constant decreases remarkably upon aggregation, which further induces strong solid fluorescence. To unravel the intrinsic mechanism, we focus on two important factors of k_{ic} including non-adiabatic coupling and reorganization energy.[32] We made a detailed analysis of the change in non-adiabatic coupling from Figure 3a, and it can be seen that the couplings become much smaller from solution to solid phase. In solution, the low-frequency vibrations of 22.49, 74.16, 97.08, and 116.33 cm^{-1} have large non-adiabatic couplings, and these modes all belong to the bending vibrations of bond C—Cu—Cl. On the contrary, these kind of vibrations are significantly suppressed in solid phase; only the modes of 65.10 cm^{-1} make a much smaller contribution. What's more, the total reorganization energies decrease a lot from solution (7,121 cm^{-1}) to solid state (2,274 cm^{-1}), and it can be seen from Figure 3b that the largest contributions to the reorganization energy come from several low-frequency modes. These low-frequency modes are assigned to the bending vibrations associated with coordination bonds C1—Cu and Cu—Cl from the displacement vectors in Figure 3b. We further established the structure–property relationship by projecting the reorganization energies onto the internal coordinates as shown in Figure 3c. It is obvious that the bond angles Cu—C1—N, C1—Cu—Cl, and Cu—C1—C4 are the most sensitive parameters to the environment. The coordinate bond angle vibrations provide the major contribution to

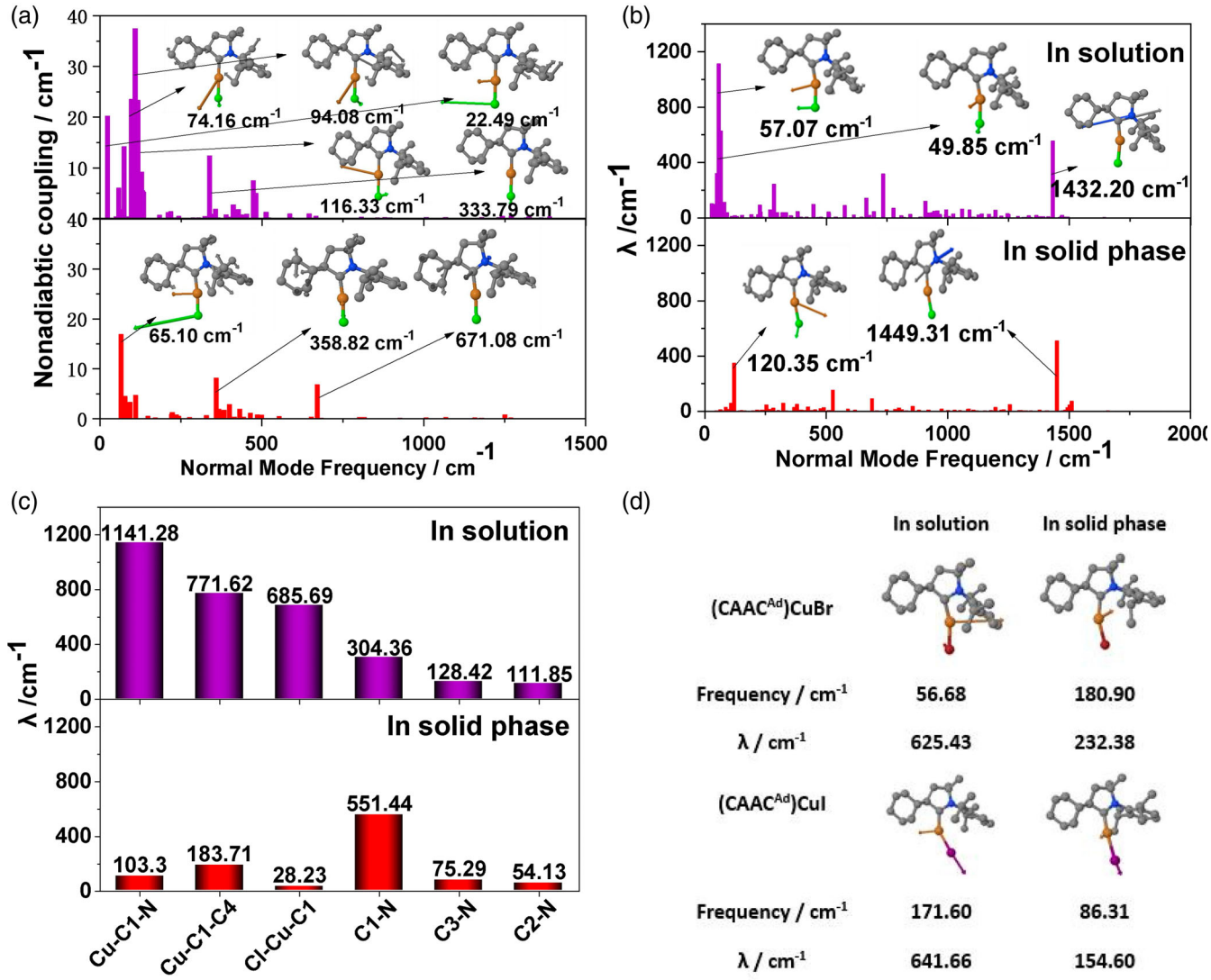

FIGURE 3 (a) Diagonal elements of the electronic non-adiabatic coupling matrix R_{ll} for (CAAC^{Ad})CuCl in solution (purple) and solid phases (red); (b) reorganization energy (λ) contributed from normal mode (CAAC^{Ad})CuCl; (c) projection of the total reorganization energy onto the internal coordinates relation for solution and solid phases; (d) The selected modes with reorganization energy (λ) of (CAAC^{Ad})CuBr and (CAAC^{Ad})CuI in solution and solid phase. Reproduced with permission from ref. [17]. Copyright 2019 American Chemical Society

the reorganization energy in solution, while their contributions vanish in solid phase. The change of the reorganization energy again leads to a great decrease of the non-radiative decay rate upon aggregation. The universality of the luminescence mechanism of the two-coordinate Cu(I) complexes with similar chemical structures is confirmed by exploring the photophysical properties of (CAAC^{Ad})CuBr and (CAAC^{Ad})CuI as shown in Figure 3d. Herein, the low-frequency bending vibrations are also significantly restricted upon aggregation, which leads to smaller reorganization energy in solid phase.

Overall, the strong solid-state fluorescence is induced by the restriction of the bending vibrations of the coordination bonds for the complex (CAAC^{Ad})CuCl. In other words, restriction of Renner–Teller distortion will benefit the enhancement of the luminescent efficiency, and this molecular design principle has been successfully applied in carbene-Au(I)-aryl complexes.[33] This is quite different from the traditional AIE caused by the restriction of rotational,[34] twisting,[35] and stretching[36] vibrations.

3 | MECHANISM OF AGGREGATION-ENHANCED TADF IN TWO-COORDINATE Cu(I) COMPLEX

Two-coordinate Carbene-Metal-Amide (CMA) complexes have been demonstrated to have outstanding TADF performance, which attracts increasing attention,[3] shown

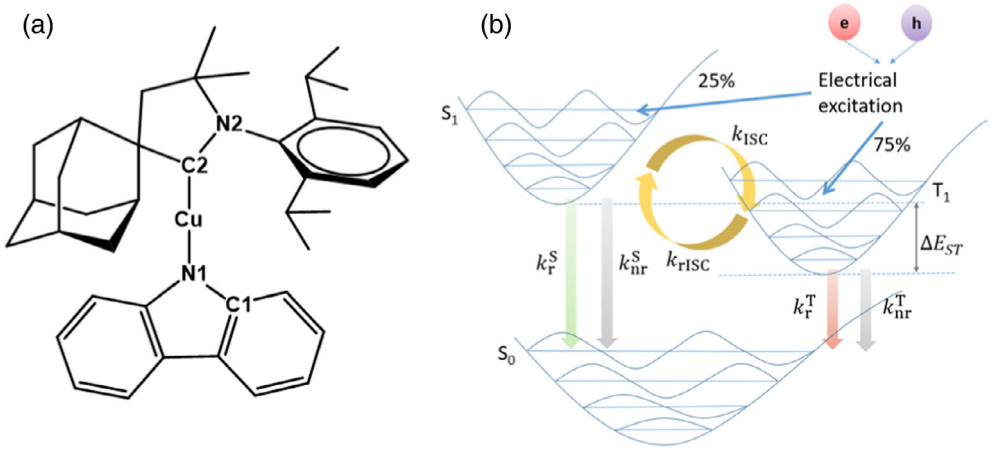

FIGURE 4 (a) Chemical structure of CAAC—Cu(I)—Cz; (b) Excited state decay processes for TADF, consisting of radiative (k_r^S) and non-radiative (k_{nr}^S) decay from S_1 to S_0, radiative (k_r^T) and non-radiative (k_{nr}^T) decay from T_1 to S_0, ISC (k_{ISC}) and rISC (k_{rISC}) between S_1 and T_1. Reproduced with permission from ref. [27]. Copyright 2021 American Chemical Society

TABLE 2 Calculated rate constants (s^{-1}) of the excited state decay processes and TADF quantum efficiency for CAAC—Cu(I)—Cz in both chlorobenzene solution and solid phase, as well as the available experimental data

	k_r^S	k_{nr}^S	k_r^T	k_{nr}^T	k_{ISC}	k_{rISC}	$k_{r,avg.}$	ϕ_{TADF}
CAAC—Cu(I)—Cz								
Solution	1.76×10^7	2.51×10^4	2.15×10^1	1.16×10^4	1.52×10^8	4.51×10^5	6.58×10^4 (3.0×10^5)[a]	72% (68%)[a]
Solid	2.05×10^7	7.07×10^3	1.04×10^1	1.61×10^4	5.64×10^{10}	1.74×10^9	2.75×10^5	97%

Source: Reproduced with permission from ref. [24]. Copyright 2021 American Chemical Society.
[a]Available experimental data measured in 2-Me-THF in Ref. [3].

in Figure 4a. However, the understanding of the high TADF efficiency mechanism for CMA complexes has aroused widespread controversies. A number of mechanisms have been proposed in both experimental and theoretical works, including rotationally accessed spin-state inversion (RASI),[3] fast up-conversion process at coplanar geometry[37] and CMA bond deformation induce TADF.[38] However, these mechanisms are based on single molecule, and the aggregation effect was yet to be determined. Especially, for the (reverse) intersystem crossing processes (Figure 4b), the aggregate effects should be explored with caution.

We obtained the equilibrium geometries and frequencies of ground and excited state in (TD)M06/6-31G(d)/LANL2DZ level with PCM (chlorobenzene) for the solvent effect and QM/MM model for crystal environment. All these electronic structure calculations were carried out in *Gaussian 16* package.[30] And then, we systematically calculated the rates for the involved radiative, non-radiative and ISC/rISC rates of CAAC—Cu(I)—Cz in solution and solid phase using our self-developed TVCF formalism implemented in MOMAP package.[26] The results of rate constants are presented in Table 2, in comparison with the available experimental data. It is seen that the k_{ISC} and k_{rISC} are most sensitive to the environment among all the rate constants, which increases sharply by several orders of magnitude from solution to solid phase (from 1.52×10^8 s^{-1} and 3.16×10^8 s^{-1} in solution to 5.64×10^{10} s^{-1} and 6.23×10^{10} s^{-1} in aggregates, respectively). The non-radiative rate constants (k_{nr}^S) decreases one order of magnitude upon aggregation, which efficiently enhances the luminescence in aggregate. Based on these rate constants, we calculated the averaged radiative rate constants by the following equation as $k_{r,avg.} = [k_r^T + k_r^S \exp(-\Delta E_{ST}/k_B T)]/[3+\exp(-\Delta E_{ST}/k_B T)]$,[39] and we got the $k_{r,avg.}$ as 6.58×10^4 s^{-1} in solution of CAAC—Cu(I)—Cz, which conforms to the experimental result (3.0×10^5 s^{-1}). The overall TADF quantum efficiencies (ϕ_{TADF}) can be evaluated as $\phi_{TADF} = \phi_{PF}[\phi_{ISC}\phi_{rISC}/(1-\phi_{ISC}\phi_{rISC})]$, where $\phi_{ISC} = [k_{ISC}/(k_{ISC}+k_r^S+k_{nr}^S)]$, $\phi_{rISC} = [k_{rISC}/(k_{rISC}+k_r^T+k_{nr}^T)]$, and the prompt fluorescence $\phi_{PF} = k_r^S/(k_{ISC}+k_r^S+k_{nr}^S)$.[40] The resultant ϕ_{TADF} of CAAC—Cu(I)—Cz is 72% in solution, which is again in good agreement with experimentally measured 68%, and enhanced to 98% upon aggregation, which brings up exceptional OLEDs performance in application.

Based on the optimized geometries of ground and excited states, we found that for CAAC—Cu(I)—Cz the T_1 optimized geometry becomes more bent with angle ∠C2—Cu—N1 decreasing from 173.7° to 166.3° upon aggregation. The geometrical change of T_1 subsequently affects the electronic structure as Figure 5 shown. Upon aggregation, the Cu component of frontier molecular orbital (FMO) is considerably increased at the T_1 optimized geometry while almost unchanged at S_0 and S_1

TABLE 3 Calculated energy gap (ΔE_{ST}) and activation energy (ΔG), spin-orbit coupling (ξ), reorganization energy ($\lambda_{T1\rightarrow S1}$) for the transition from $T_1 \rightarrow S_1$, reorganization energy ($\lambda_{S1\rightarrow T1}$) for the transition from $S_1 \rightarrow T_1$ and the contribution of metal atom to spin-orbit coupling (ξ_{S1T1}) for CAAC—Cu(I)—Cz in both solution and solid phases

	ΔE_{ST} (eV)	ξ_{S1T1} (cm^{-1})	ξ_{Metal} (cm^{-1})	$\lambda_{T1\rightarrow S1}$ (cm^{-1})	$\lambda_{S1\rightarrow T1}$ (cm^{-1})	ΔG_{ISC} (eV)	ΔG_{RISC} (eV)
Solution	0.12 (0.07)[a]	1.84	1.32	151	151	0.14	0.26
Solid	0.08	7.35	7.57	530	647	0.01	0.08

Source: Reproduced with permission from ref. [24]. Copyright 2021 American Chemical Society.
[a]Vertical ΔE_{ST} calculated in gas phase at T_1 optimized geometry at TDA-PBE0/def2-SVP by ref. [36].

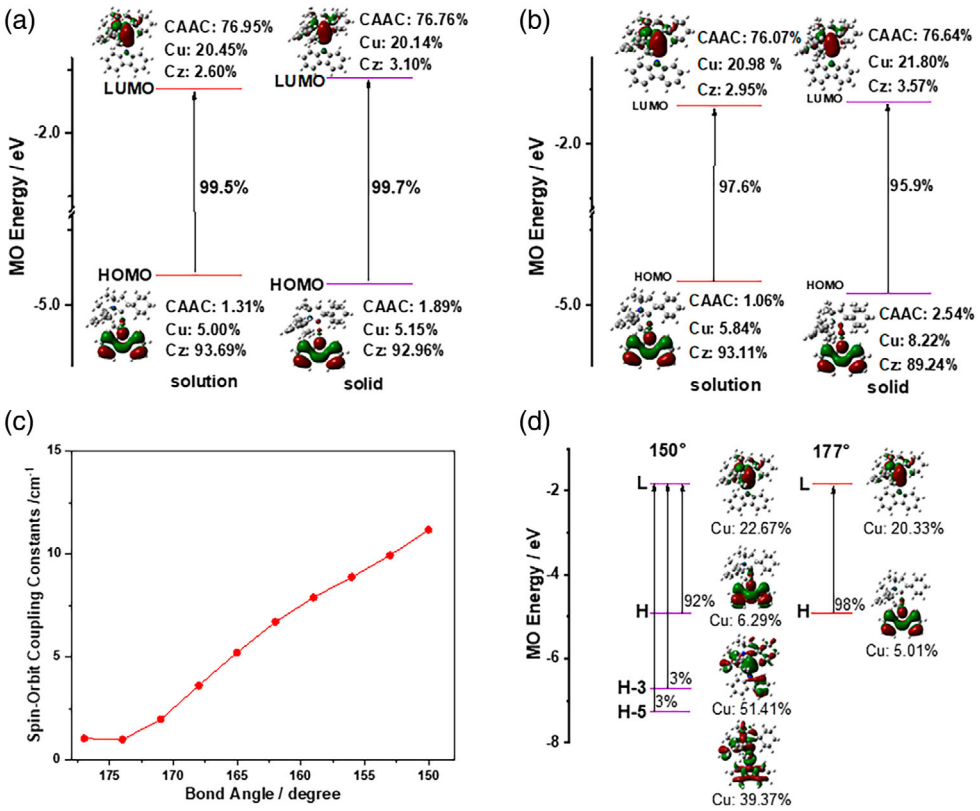

FIGURE 5 Energy level and composition analysis for the selected frontier orbitals for S_1 and T_1 state at S_1-geometries and T_1-geometries of CAAC—Cu(I)—Cz (a,c) and CAAC—Au(I)—Cz (b,d), respectively. Reproduced with permission from Ref. [24]. Copyright 2021 American Chemical Society

optimized geometries due to the bent structure of T_1. We scanned the potential energy surface (PES) of T_1 along ∠C2—Cu—N1 to unravel the relationship between the SOC and coordinate bond angle, and calculated the SOC between S_1 and T_1 of every single point shown as in Figure 5c. It is found that ξ_{S1T1} increased monotonously from 1.04 to 11.1 cm^{-1} with the decrease of ∠C2—Cu—N1 from 178° to 150°. The larger contributions of Cu atom in the bent T_1 optimized geometry resulted from the Renner–Teller distortion, which is not uncommon in linear d^{10} coinage complexes (Figure 5d). Consequently, the transition MLCT character becomes more significant, which improves the SOC due to heavy atom effect and facilitates the occurrence of ISC/rISC process.

In principle, rISC process is determined by three key factors: singlet-triplet energy gap (ΔE_{ST}), SOC (ξ), and activation energy between the S_1 and T_1 states. The calculated values and related reference data are listed in Table 3. The adiabatic ΔE_{ST} significantly decreases from 0.12 to 0.08 eV for CAAC—Cu(I)—Cz, because of the larger increase of the T_1 with respect to S_1. And the calculated SOC between S_1 and T_1 states becomes much stronger from solution (1.84 cm^{-1}) to solid state (7.35 cm^{-1}), which could be attributed to the increased contribution from the metal atomic orbitals from 1.32 to 7.57 cm^{-1} due to the Renner–Teller distortion.

Furthermore, λ_{S1T1} increases a few fold upon aggregation as shown in Table 3. The activation energy can be expressed as $\Delta G = (-\Delta E_{if} + \lambda)^2/4\lambda$ according to Marcus theory,[41] which is the energy barrier for the ISC/rISC process. Because of the reduced ΔE_{ST} and increased λ_{S1T1}, ΔG drops from 0.14/0.26 eV in solution to 0.01/0.08 eV in aggregate for ISC/rISC for CAAC—Cu(I)—Cz, accelerating both ISC and rISC processes. Through the

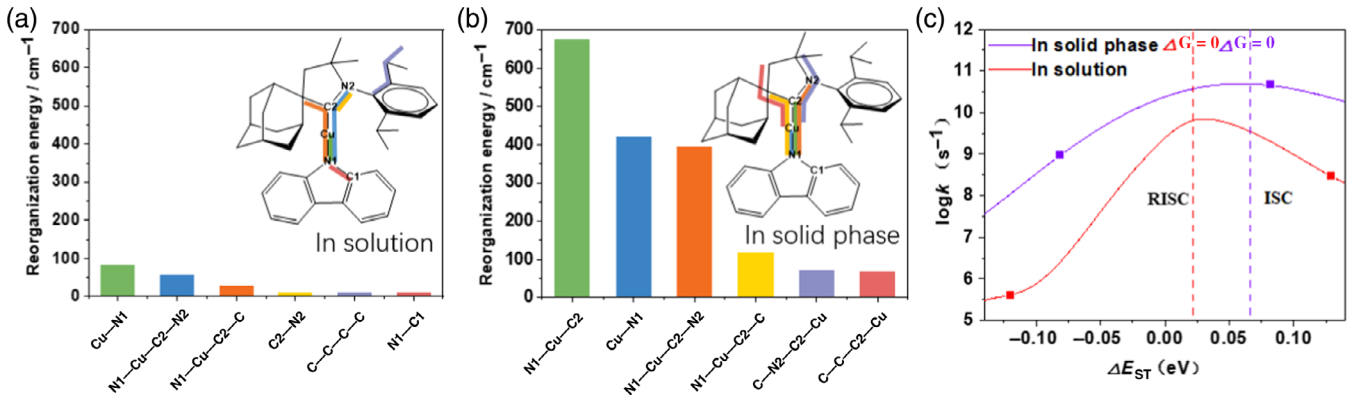

FIGURE 6 The reorganization energy between S_1 and T_1 states and projections onto the internal coordinates for CAAC—Cu(I)—Cz (a) in solution and (b) solid phase; (c) intersystem crossing rate constant as a function of energy gap of CAAC—Cu(I)—Cz. Reproduced with permission from ref. [24]. Copyright 2021 American Chemical Society

projection of reorganization energies between S_1 and T_1 onto the internal coordinates for CAAC—Cu(I)—Cz (Figure 6a,b), we found that λ_{S1T1} mainly comes from the stretching vibration of Cu—N (Au—N) bond and the bending vibration of coordinate bonds with angles C—Cu—N or C—Au—N. In other words, it is the Renner–Teller distortion related to metal, causing large reorganization energy in solid phase and accelerating both the ISC and rISC transitions.

In order to disclose the dependence of the key factors and ISC/rISC rate constants on aggregation, Figure 6c depictes k_{ISC} and k_{rISC} as a function of energy gap. The actual situation occurs when gap equals to ΔE_{ST}. The rate reaches up to the maximum when $\Delta G = 0$ at $\Delta E = \lambda$. The synergestic effect of increasing SOC and decreasing ΔG from solution to aggregates gives rise to the aggregation-induced TADF through accelerating both ISC and rISC rates (see Figure 6).

To summarize this part, ϕ_{TADF} enhancement from 72 to 97% for CAAC—Cu(I)—Cz upon aggregation, owing to the 2–4 orders of magnitudes increased ISC and rISC rate constants. Increase of ISC/rISC rate constants in solid states mainly stems from the increased SOC and reduced activation energy (induced by increased reorganization energy and decreased ΔE_{ST}). Our systematical investigation of the TADF mechanism of CAAC—Cu(I)—Cz would help for the designation of novel highly efficient copper complexes.

4 | CONCLUSIONS AND PERSPECTIVES

In conclusion, we have comprehensively studied the photophysical properties of two-coordinate Cu(I) complexes in both solution and solid states by PCM and QM/MM methods coupled with TVCF rate formalism developed by our group. Through systematically analysis of the electronic structures, reorganization energy, non-adiabatic coupling, and the excited-state decay rates in the two phases, we have revealed the mechanism of highly efficient solid-state fluorescence and TADF of two-coordinate Cu(I) complexes.

First, we investigated the aggregation effect on the photophysical properties of CAAC—Cu(I)—Cl complex. Computational results revealed that the transition properties changed from MLCT in solution to hybrid XLCT and MLCT in solid state. The bending vibrations of the C—Cu—Cl and Cu—C—N bonds are largely restricted in aggregates, which reduced the non-radiative decay and induced strong solid-state fluorescence. This theoretical study provides a clear rationalization for the highly efficient fluorescence character of two-coordinate Cu(I) complexes.

Second, we studied the photophysical properties of CAAC—Cu(I)—Cz in solution phase in close comparison to solid phase. We found that both ISC and RISC rates were enhanced by 2–4 orders of magnitude upon aggregation, leading to highly efficient TADF. The enhanced ISC and RISC rates could be attributed to a synergistic effect of increase in spin−orbit coupling between S_1 and T_1, due to increased metal proportion in the FMOs, and the decrease of the reaction barriers for ISC and RISC due to increased reorganization energy through the bending angle ∠C—Cu—N for T_1. These findings can clarify the ongoing dispute on the understanding of the high TADF quantum efficiency for the two-coordinate metal complexes.

Metal coordinated organic molecules or polymers have also been demonstrated highly interesting thermoelectric conversion properties.[42] Although the copper complex luminescent materials have been developed for several decades, there are still a number of unsolved problems. In our work, we have discovered the important role of Renner–Teller distortion played in prompt

fluorescence and TADF excited state decay process of two-coordinate Cu(I) complexes, especially for the non-radiative decay process, while the mechanism of phosphorescent emission is yet to be disclosed. Besides, the AIE phenomena are widely reported in Cu(I) complex, but a comprehensive understanding of the luminescence mechanism is urgently required due to the multiplicity of coordination forms. Furthermore, the Cu(I) complexes can present prompt fluorescence, delayed fluorescence, and phosphorescence. It is not fully understood how to realize the conversion of this behavior through molecular design. Our computational rationalizations for the exotic photophysical processes are the first step for molecular design to achieve targeted luminescence.

ACKNOWLEDGMENTS

It is with great sadness to learn that Professor Sheng-Hsien Lin passed away. He is a giant and pioneer of the theory of molecular radiationless decay. The first time I met him was during a conference he organized in Taipei in 2002 when I presented theory of beating the 25% spin statistical limit for polymer electroluminescence. The next year, he came to Beijing to attend a conference I organized to present a plenary lecture. Since then, we constantly met and discussed issues of common interests. It was under his constant encouragement that we have made some progress in understanding the luminescent and transport properties of molecular materials. We will miss Professor Sheng-Hsien Lin but we will never forget him. This work is supported by the National Natural Science Foundation of China Grant Nos. 21788102 and 22003030, as well as by the Ministry of Science and Technology of China through the National Key R&D Plan, Grant No. 2017YFA0204501.

ORCID

Qi Ou https://orcid.org/0000-0002-6400-7522

REFERENCES

[1] F. Dumur, *Org. Electron.* **2015**, *21*, 27.
[2] H. Yersin, *Highly Efficient OLEDs: Materials Based on Thermally Activated Delayed Fluorescence*, Wiley-VCH, Weinheim **2018**.
[3] D. Di, A. S. Romanov, L. Yang, J. M. Richter, J. P. H. Rivett, S. Jones, T. H. Thomas, M. Abdi Jalebi, R. H. Friend, M. Linnolahti, M. Bochmann, D. Credgington, *Science* **2017**, *356*, 159.
[4] G. Blasse, D. R. McMillin, *Chem. Phys. Lett.* **1980**, *70*(1), 1.
[5] J. Luo, Z. Xie, J. W. Y. Lam, L. Cheng, H. Chen, C. Qiu, H. S. Kwok, X. Zhan, Y. Liu, D. Zhu, B. Z. Tang, *Chem. Commun.* **2001**, *18*, 1740.
[6] D. Oelkrug, A. Tompert, J. Gierschner, H.-J. Egelhaaf, M. Hanack, M. Hohloch, E. Steinhuber, *J. Phys. Chem. B* **1998**, *102*(11), 1902.
[7] Y. Hong, J. W. Y. Lam, B. Z. Tang, *Chem. Soc. Rev.* **2011**, *40*(11), 5361.
[8] H. Yersin, W. J. Finkenzeller, *Highly Efficient OLEDs With Phosphorescent Materials*, Wiley-VCH, Weinheim **2007**.
[9] X. Zhang, D. Jacquemin, Q. Peng, Z. Shuai, D. Escudero, *J. Phys. Chem. C* **2018**, *122*(11), 6340.
[10] N. Armaroli, G. Accorsi, F. Cardinali, A. Listorti, in *Photochemistry and Photophysics of Coordination Compounds I* (Eds: V. Balzani, S. Campagna), Springer Berlin Heidelberg, Berlin, Heidelberg **2007**, p. 69.
[11] A. S. Romanov, D. Di, L. Yang, J. Fernandez-Cestau, C. R. Becker, C. E. James, B. Zhu, M. Linnolahti, D. Credgington, M. Bochmann, *Chem. Commun.* **2016**, *52*, 6379.
[12] V. A. Krylova, P. I. Djurovich, B. L. Conley, R. Haiges, M. T. Whited, T. J. Williams, M. E. Thompson, *Chem. Commun.* **2014**, *50*, 7176.
[13] R. Czerwieniec, M. J. Leitl, H. H. H. Homeier, H. Yersin, *Coord. Chem. Rev.* **2016**, *325*, 2.
[14] L.-P. Liu, Q. Li, S.-P. Xiang, L. Liu, X.-X. Zhong, C. Liang, G. H. Li, T. Hayat, N. S. Alharbi, F.-B. Li, N.-Y. Zhu, W.-Y. Wong, H.-M. Qin, L. Wang, *Dalton Trans.* **2018**, *47*, 9294.
[15] R. Hamze, J. L. Peltier, D. Sylvinson, M. Jung, J. Cardenas, R. Haiges, M. Soleilhavoup, R. Jazzar, P. I. Djurovich, G. Bertrand, M. E. Thompson, *Science* **2019**, *363*, 601.
[16] K. A. Barakat, T. R. Cundari, M. A. Omary, *J. Am. Chem. Soc.* **2003**, *125*, 14228.
[17] S. Lin, Q. Peng, Q. Ou, Z. Shuai, *Inorg. Chem.* **2019**, *58*, 14403.
[18] J. C. Deaton, S. C. Switalski, D. Y. Kondakov, R. H. Young, T. D. Pawlik, D. J. Giesen, S. B. Harkins, A. J. M. Miller, S. F. Mickenberg, J. C. Peters, *J. Am. Chem. Soc.* **2010**, *132*, 9499.
[19] M. Caricato, B. Mennucci, J. Tomasi, F. Ingrosso, R. Cammi, S. Corni, G. Scalmani, *J. Chem. Phys.* **2006**, *124*(12), 124520.
[20] A. Warshel, M. Levitt, *J. Mol. Biol.* **1976**, *103*, 227.
[21] Z. Shuai, *Chin. J. Chem.* **2020**, *38*, 1223.
[22] Y. L. Niu, Q. Peng, Z. G. Shuai, *Sci. China Ser. B Chem.* **2008**, *51*, 1153.
[23] Q. Peng, Y. Niu, Q. Shi, X. Gao, Z. Shuai, *J. Chem. Theory Comput.* **2013**, *9*, 1132.
[24] S. H. Lin, *J. Chem. Phys.* **1966**, *44*, 3759.
[25] S. H. Lin, C. H. Chang, K. K. Liang, R. Chang, J. M. Zhang, T. S. Yang, M. Hayashi, Y. J. Shiu, F. C. Hsu, *Adv. Chem. Phys.* **2002**, *121*, 1.
[26] Y. Niu, W. Q. Li, Q. Peng, H. Geng, Y. P. Yi, L. J. Wang, G. J. Nan, D. Wang, Z. Shuai, *Mol. Phys.* **2018**, *116*, 1078.
[27] S. Lin, Q. Ou, Y. Wang, Q. Peng, Z. Shuai, *J. Phys. Chem. Lett.* **2021**, *12*(11), 2944.
[28] F. Maseras, K. Morokuma, *J. Comput. Chem.* **1995**, *16*, 1170.
[29] Š. Budzák, M. Medved', B. Mennucci, D. Jacquemin, *J. Phys. Chem. A* **2014**, *118*, 5652.
[30] M. Frisch, G. Trucks, H. Schlegel, G. Scuseria, M. Robb, J. Cheeseman, G. Scalmani, V. Barone, G. Petersson, H. Nakatsuji, *Gaussian 16*, Gaussian Inc., Wallingford, CT **2016**, p. 2016.
[31] Y. Shao, Z. Gan, E. Epifanovsky, A. T. Gilbert, M. Wormit, J. Kussmann, A. W. Lange, A. Behn, J. Deng, X. Feng, *Mol. Phys.* **2015**, *113*, 184.
[32] Z. Shuai, Q. Peng, *Phys. Rep.* **2014**, *537*, 123.
[33] T. Y. Li, D. S. Muthiah Ravinson, R. Haiges, P. I. Djurovich, M. E. Thompson, *J. Am. Chem. Soc.* **2020**, *142*(13), 6158.
[34] T. Zhang, Q. Peng, C. Quan, H. Nie, Y. Niu, Y. Xie, Z. Zhao, B. Z. Tang, Z. Shuai, *Chem. Sci.* **2016**, *7*, 5573.

[35] F. Bu, R. Duan, Y. Xie, Y. Yi, Q. Peng, R. Hu, A. Qin, Z. Zhao, B. Z. Tang, *Angew. Chem.* **2015**, *54*, 14492.
[36] H. Ma, W. Shi, J. J. Ren, W. Li, Q. Peng, Z. Shuai, *J. Phys. Chem. Lett.* **2016**, *7*(15), 2893.
[37] J. Föller, C. M. Marian, *J. Phys. Chem. Lett.* **2017**, *8*, 5643.
[38] E. J. Taffet, Y. Olivier, F. Lam, D. Beljonne, G. D. Scholes, *J. Phys. Chem. Lett.* **2018**, *9*, 1620.
[39] W. P. To, D. Zhou, G. S. M. Tong, G. Cheng, C. Yang, C.-M. Che, *Angew. Chem. Int. Ed.* **2017**, *56*, 14036.
[40] Q. Peng, D. Fan, R. Duan, Y. Yi, Y. Niu, D. Wang, Z. Shuai, *J. Phys. Chem. C* **2017**, *121*, 13448.
[41] L. Wang, Q. Ou, Q. Peng, Z. Shuai, *J. Phys. Chem. A* **2021**, *125*, 1468.
[42] R. Liu, Y. Ge, D. Wang, Z. Shuai, *CCS Chem.* **2021**, *3*, 1477.

AUTHOR BIOGRAPHIES

Shiyun Lin was born in 1995 in Zhangzhou, Fujian Province, China. She received her BSc degree in Chemistry from Beijing Normal University in 2017. She obtained her PhD in Chemistry from Tsinghua University in 2022, supervised by Prof Zhigang Shuai. Her research interests focus on theoretical investigations into the molecular aggregation effects of organic luminescent materials with TADF properties and computational selection of organic laser materials.

Qi Ou was born in 1989 in Beijing, China. She received her BSc degree in Chemistry from the University of Science and Technology of China. In 2017, she obtained her PhD in Chemistry from the University of Pennsylvania, working with Prof Joseph Subotnik. After postdoctoral research with Prof Emily Carter at Princeton University and Prof Zhigang Shuai at Tsinghua University, she became a research scientist in AI at the Science Institute, Beijing. Her research centers on the development of electronic structure tools for molecular systems (especially excited states) and rate theories for photophysical processes, as well as the development of machine-learning based density functionals for periodic systems.

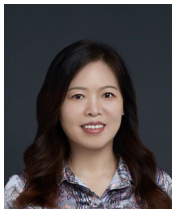

Qian Peng received her PhD from the Institute of Chemistry of the Chinese Academy of Sciences in 2008, supervised by Prof Z. Shuai. Then she joined the Key Laboratory of Organic Solids at the Institute as a research assistant, and she was promoted to associate professor in 2010 and to full professor in 2019. In 2020, she joined the School of Chemical Sciences, University of Chinese Academy of Sciences in Beijing. Her research interests are theoretical investigations into the molecular aggregation effects on light-emitting phenomena with excited-state decay processes involving nonadiabatic and spin−orbit couplings, photophysical mechanisms of various luminescence phenomena in organic optoelectronic materials, and the theoretical design of light-emitting molecules.

Zhigang Shuai received BSc in 1983 from Sun Yat-sen University and his PhD in 1989 from Fudan University. He went to work with Prof Jean-Luc Brédas as a postdoc at the University of Mons, Belgium. In 2000, he received the support of the "Hundred-Talent Program" in the Institute of Chemistry of the Chinese Academy of Sciences. He was granted the Outstanding Young Investigator's Fund by the National Natural Science Foundation of China in 2004. He moved to Tsinghua University in 2008 as a Changjiang Scholar Chair Professor. He has been working on developing a computational method for modeling and understanding the electronic processes in organic and polymeric materials, focusing on the excited state structure and dynamics. His computational package, MOMAP, has been successfully commercialized. He has published more than 440 papers in scientific peer-reviewed journals, with more than 24,000 citations (H-index 85). He has been elected as a member of the International Academy of Quantum Molecular Science in 2008, a Fellow of the Royal Society of Chemistry in 2009, a foreign member of the Academia Europaea in 2011, an associate member of the Royal Academy of Belgium in 2013, a board member of the World Association of Theoretical and Computational Chemists (WATOC) in 2017, and a member of the IUPAC executive committee in 2022. He is also an Honorary Member of the Physical Society of Uzbekistan and a Fellow of the Chinese Chemical Society. He was the recipient of the Chinese Chemical Society—AkzoNobel Chemical Science Award (2012), the French Chemical Society Prix Franco-Chinois (2018), and the First-Class Award of the Beijing Municipal Natural Science Prize (2020).

How to cite this article: S. Lin, Q. Ou, Q. Peng, Z. Shuai, *J. Chin. Chem. Soc.* **2023**, *70*(3), 287. https://doi.org/10.1002/jccs.202200347